Kinetics and Catalysis, Vol. 44, No. 3, 2003, pp. 432–440. Translated from Kinetika i Kataliz, Vol. 44, No. 3, 2003, pp. 471–480.

VI RUSSIAN CONFERENCE ON CATALYTIC REACTION MECHANISMS (Moscow, October 1–5, 2002)

The Nature of Electrophilic and Nucleophilic Oxygen Adsorbed on Silver

V. V. Kaichev*, V. I. Bukhtiyarov*, M. Hävecker, A. Knop-Gercke**, R. W. Mayer**, and R. Schlögl****

** Boreskov Institute of Catalysis, Siberian Division, Russian Academy of Sciences, Novosibirsk, 630090 Russia*

*** Fritz-Haber-Institut der Max-Planck-Gesellschaft, Berlin, Germany*

Received December 17, 2002

Abstract—Results of a spectroscopic study of two forms of adsorbed atomic oxygen on a silver surface, which participate in ethylene epoxidation reaction, are presented. The possibility of the combined use of the methods of photoelectron spectroscopy and X-ray absorption for a detailed analysis of adsorbate electron structure on solid surfaces is demonstrated. It is found that a significant difference in the position of O 1*s* lines for nucleophilic (528.3 eV) and electrophilic (530.4 eV) oxygen is determined by the effects of the initial state, that is, by the difference in the charge state of oxygen anions. The use of the well-know correlation of the Auger line splitting with a Pauling charge at an oxygen atom showed a substantial difference (~1 electron charge unit) in charge transfer from metal to the nucleophilic or electrophilic adsorbed oxygen atom. Based on the X-ray absorption data of the oxygen *K*-edge, it is found that there is a substantial overlap of the 4*d*- and 5*sp* orbitals of silver with oxygen 2*p* orbitals in the nucleophilic state in the formation of an Ag–O bond and there is only an overlap of 5*sp* orbitals of silver with oxygen 2*p* orbitals in the electrophilic state. Structural models of the adsorption site are presented for both states. The conclusion is drawn that the charge state of oxygen in oxide systems may depend substantially on its binding to metal atoms.

INTRODUCTION

Ethylene epoxidation over silver surfaces forms the basis of a large-scale process and can be considered as one of the best studied selective oxidation reactions in heterogeneous catalysis [1–15]. Moreover, this reaction is cited as the motivation behind most of the studies devoted to oxygen adsorption on silver surfaces [16–34].

Most researchers assume that the occurrence of this reaction via complete or partial oxidation pathways is determined by the state of the silver surface and by the states of adsorbed oxygen. Thus, van Santen and coworkers [5, 6] and Grant and Lambert [7] showed that ethylene partial oxidation does not occur on clean silver. To initiate selective catalysis, preliminary treatment of silver with oxygen or with the reaction mixture at pressures of ~100 Pa is needed. A surface treated under such conditions preserves its activity even upon further evacuation. X-ray photoelectron spectroscopy (XPS) was used to determine the existence of two oxygen states on silver surfaces under reaction conditions: nucleophilic and electrophilic, with electron binding energies (E_b) at the O 1*s* level equal to 528.4 and 530.4 eV, respectively [10]. Oxygen in the former state is active in the nucleophilic attack on the C–H bond of an ethylene molecule with further oxidation to CO_2 and H_2O. The presence of both states is necessary for the occurrence of selective oxidation. It has been shown by the direct isotopic method that electrophilic oxygen is directly inserted into an ethylene molecule, whereas the nucleophilic state initiates the transition of silver atoms into the ionic Ag^+ state, which is necessary for ethylene adsorption [11].

The structure and properties of nucleophilic oxygen were characterized in detail by various methods. It was found that the nucleophilic state is readily formed on a clean silver surface via the dissociative adsorption of oxygen at 400–600 K. Silver coordination at the reconstructed surface is close to the structure of bulk oxide Ag_2O [21–24]. Oxygen in this state is highly reactive toward gases like H_2, CO, and CO_2. The nature of the electrophilic state is still actively discussed [1–15]. It is known that this state is formed upon the long treatment of silver at 400–600 K in an atmosphere of oxygen or reaction mixtures ($P = 10^{-2}$–10^3 Pa). Angle-resolved XPS with the use of the method of layer-by-layer analysis showed the surface localization of the electrophilic state [10, 17]. It was confirmed in several papers that the electrophilic state is atomic adsorbed oxygen [13–15] and the O–O bonds are absent from the structure of the adsorption complex. Note that, in *in situ* experiments under conditions close to real catalysis (a reaction mixture pressure of 200 Pa and a temperature of 470 K), additional (weakly adsorbed) states of adsorbed oxygen have not been found on the silver surface [14].

0023-1584/03/4403-0432$25.00

Thus, analysis of literature data suggests that there are two adsorbed oxygen states on the silver surface, which display nucleophilic and electrophilic properties in ethylene oxidation. Substantial differences in the positions of framework O 1*s* levels assume the difference in the charge states of oxygen anions in the nucleophilic and electrophilic states. To construct a detailed mechanism of ethylene epoxidation and determine the reason for the uniqueness of silver as a catalyst for this reaction, it is necessary to determine the specific features of the electron structure of these two adsorption states. At the same time, the experimental proof for the existence of atomic oxygen adsorption states with different electron structures is important from the standpoint of creating the phenomenological basis for developing the concept of the effect of metal–oxygen charge-transfer processes on the pathways of catalytic oxidation reactions.

In this paper, we report the results of a spectroscopic study of nucleophilic and electrophilic states of oxygen adsorbed on the silver surface. We determined the specific features of the Ag–O interaction resulting in different reactivities of these states in ethylene epoxidation. We also demonstrate the possibility of studying the electron structure of adsorbates on solid surfaces using a unit of complementary methods: X-ray absorption spectroscopy and photoelectron spectroscopy.

EXPERIMENTAL

XPS experiments were carried out using an ultrahigh vacuum VG ESCALAB HP spectrometer. Its construction and the main characteristics were reported earlier in detail [35, 36]. The vacuum part of the setup consists of an analytical chamber and two preparation chambers, each having an independent pump spool and a system for gas admission. A convenient system of locking and sample holder enabled treatment with reaction mixtures in the preparation chamber at pressures of up to 10^5 Pa, fast (<1 min) evacuation, and transportation of a sample to the analytical chamber. The residual pressure of gases was at most 5×10^{-7} Pa. In addition to XPS (AlK_α and MgK_α radiation), the above spectrometer provides the following methods: ultraviolet photoelectron spectroscopy (UPS), temperature-programmed desorption (TPD), electron Auger spectroscopy, and low-energy electron diffraction (LEED). To calibrate the scale of binding energies of the photoelectron spectrometer, we used the Ag $3d_{5/2}$ line (E_b = 368.2 eV) in the spectrum of a clean silver surface. The use of an original system of data collection makes it possible to control synchronously the photoelectron spectrometer, quadrupole mass spectrometer, and the unit of sample heating [13, 37].

X-ray absorption near-edge structure (XANES) studies were carried out using an HE-TGM1 storage ring (Berlin synchrotron radiation source BESSY-1). The construction of the XANES spectrometer was described in detail in [38]. The vacuum part of the setup consisted of two chambers: one is for sample treatment with reaction mixtures at high pressures, and the other is for analytical measurements (the pressure of residuum gases is $\sim 5 \times 10^{-7}$ Pa). The use of a high-pressure cell makes it possible to carry out studies at high pressures (up to 2000 Pa) in the *in situ* regime. The original construction of the spectrometer allowed us to use mild X-ray radiation ($h\nu$ < 1 keV). Note in this range the absorption edges of several light elements (C, O, N, and others) are positioned. These elements play an important role in the catalytic reactions. In the course of the experiment, three signals change simultaneously: the absorption spectrum of the gas phase, the overall absorption signal at the surface and in the gas phase, and the intensity of the inlet SI radiation. The X-ray absorption spectra of carbon and oxygen *K*-edges were recorded in the regime of complete photocurrent with an accelerating voltage of +4.5 V. The spectral resolution in the range 250–1000 eV is 1.8 eV. To calibrate the photon energy scale, we used the π-resonance signal in the spectrum of molecular oxygen in the gas phase (530.8 eV).

The XPS and XANES studies of spectroscopic properties of oxygen adsorbed on silver were carried out using the same sample (silver Goodfellow foil, with 99.95% purity) under identical experimental conditions. The silver surface was preliminarily cleaned directly in the spectrometer using a cycle of treatments, including etching with argon ions with an energy of 2 keV for 10 min, heating to 800–900 K, treatment in oxygen at T = 400–500 K, and annealing in a vacuum at T = 800–900 K. After multiple treatments, the surface did not contain any admixtures (the purity of the surface was controlled by XPS, TPD, and XANES).

The spectral properties of nucleophilic oxygen were studied *in situ* at an oxygen pressure of 10^{-2} Pa and 470 K. The choice of this regime is determined by the high reactivity of nucleophilic oxygen toward background gases H_2 and CO. In *ex situ* experiments, even under "clean-off" ultrahigh vacuum conditions, the reaction leads to a fast decrease in the surface coverage by oxygen, which complicates the analysis of the adsorption layer by spectroscopic methods that require a long time for spectrum recording. A relatively high temperature of adsorption was chosen to exclude the accumulation of carbonates on the silver surface, which can readily be formed as a result of the interaction of adsorbed oxygen and background CO_2. The temperature of carbonate group decomposition was 420 K [18, 19].

The spectroscopic study of electrophilic oxygen was carried out *ex situ* after the treatment of silver foil by the reaction mixture $C_2H_4 + O_2$ (P = 200 Pa) at 470 K for 1 h. Such treatment leads to the appearance of a narrow signal with E_b = 530.4 eV in the O 1*s* spectrum, pointing to the formation of electrophilic oxygen on the

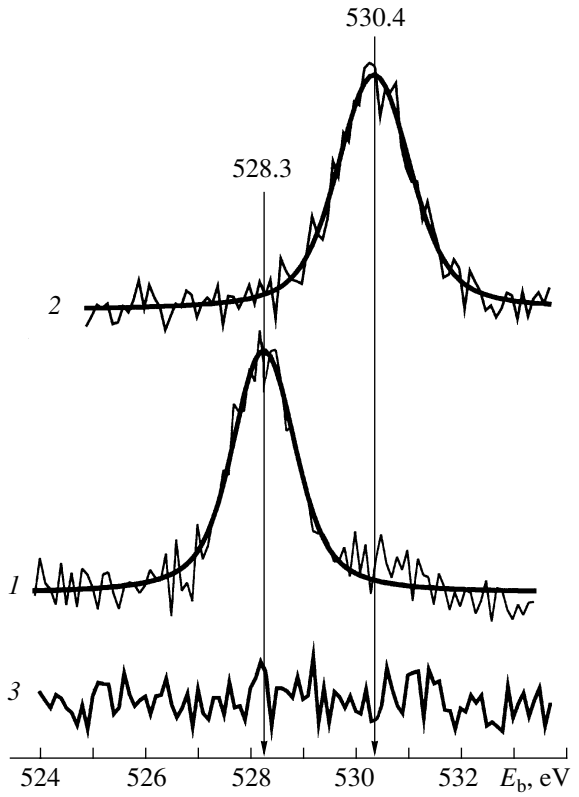

Fig. 1. XPS O 1*s* spectra of (*1*) nucleophilic and (*2*) electrophilic adsorbed oxygen and (*3*) a clean silver surface: (*1*) *in situ* in an oxygen atmosphere ($P = 10^{-2}$ Pa, $T = 470$ K); (*2*) *ex situ* after silver foil treatment with the reaction mixture at 470 K and $P = 200$ Pa (the partial pressure of ethylene is 5 Pa) for 1 h.

silver surface. The use of a low partial pressure of ethylene ($P = 5$ Pa) prevented the dissolution of a noticeable amount of reaction medium fragments in the near-surface layers of silver [13, 14].

RESULTS AND DISCUSSION

Figure 1 shows the O 1*s* spectra recorded after silver treatment with oxygen (curve *1*) and the reaction mixture (curve *2*). It is seen that, in complete agreement with our expectations and earlier data, practically individual formation of nucleophilic and electrophilic adsorbed oxygen takes place in this case. The latter follows from the appearance of the corresponding O 1*s* signals with binding energies 528.3 and 530.4 eV.

What is the reason for the apparent chemical shifts in the spectra of nucleophilic and electrophilic states and to what extent do they reflect the difference in the electron structure of adsorption complexes in the two cases? It is believed that it is the change in the charge distribution over the valence shell of an atom due to a change in the coordination and chemical bond cleavage and formation that leads to chemical shifts in the positions of binding energies of electrons at all levels. Even the first XPS studies showed that, in the compounds with similar structures, the chemical shift of inner levels of the atom is more pronounced if the effective charge at this atom is higher. When the oxidation states are negative, the shift is toward lower binding energies. In agreement with the Koopmans theorem (the approximation of frozen orbitals), the physical nature of a chemical shift can be illustrated by the point-charge model: the potential energy of the inner orbital (orbital energy) depends on the effective charge of the given atom (the potential of valence orbitals) and the charges created by the surrounding atoms [39, 40]. Note, however, that ionization excitation of an atom leads to photoelectron emission and to the formation of a vacancy at the corresponding level. The appearance of a vacancy in the course of photoemission leads to changes in wave functions of electrons in the system, which contributes noticeably to the apparent value of the binding energy. As a consequence, when analyzing chemical shifts (ΔE_B), it is necessary to take into account changes in the orbital symmetry (ΔE) and changes in the relaxation energy (ΔR):

$$\Delta E_B = -\Delta E - \Delta R. \quad (1)$$

A number of methods for estimating the relaxation energy are described in the literature. Thus, in [41–44], the concept of the Auger parameter was developed and it was shown that the difference in the Auger and photoelectron chemical shifts is due to the relaxation energies in the final states of various chemical forms:

$$\Delta\alpha = \Delta[E_A(kii) + E_B(k)] = 2\Delta R, \quad (2)$$

where α is the modified Auger parameter determined as a sum of the kinetic energy of the Auger line ($E_A(kii)$) and the binding energy of the corresponding photoelectron line ($E_B(k)$). However, in the derivation of this relation, it was assumed that the contribution of the effects of the initial state is the same for all levels participating in the Auger process, and this is not always true. The formula for determining the relaxation effect that takes into account the differences in the orbital energy of inner-shell and upper-shell electrons was proposed in [45]:

$$\Delta\beta = \Delta[2E_B(i) - E_B(k) + E_A(kii)] = 2\Delta R. \quad (3)$$

Obviously, the use of Eq. (3) for estimating the contribution of relaxation to the apparent differences in E_b of nucleophilic (O_{nucl}) and electrophilic (O_{elec}) oxygen required measuring the spectra of the valence zone and the Auger spectra of these states, which are shown in Figs. 2 and 3, respectively. (Conditions that provide the individual formation of O_{nucl} and O_{elec} are mentioned above.)

It is seen from the spectra that substantial differences are observed in the spectra of the valence zone and in the Auger spectra of the nucleophilic and electrophilic states of adsorbed oxygen. Thus, UPS spectra clearly show lines in the region of 1.9 (nucleophilic

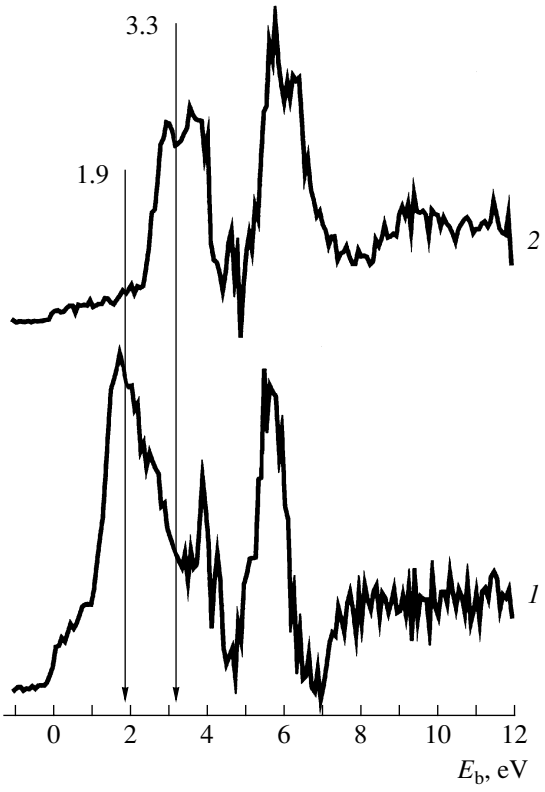

Fig. 2. Difference spectra of the valence zone of adsorbed oxygen in the (*1*) nucleophilic and (*2*) electrophilic states (after subtracting the UPS spectrum of clean silver foil); HeI radiation ($h\nu$ = 21.2 eV).

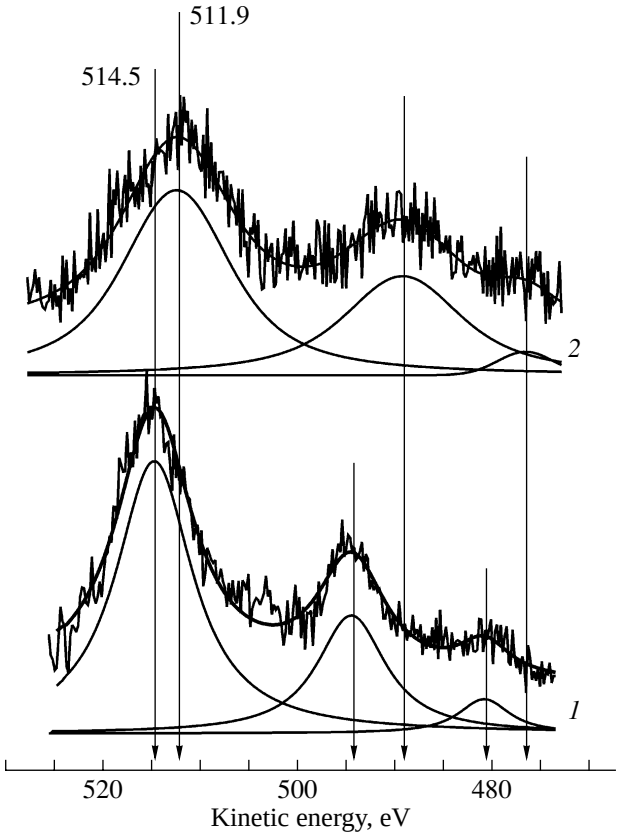

Fig. 3. Auger spectra of adsorbed oxygen in (*1*) nucleophilic and (*2*) electrophilic forms; AlK_α radiation ($h\nu$ = 1486.6 eV).

state) and 3.3 eV (electrophilic state) below the Fermi level (Fig. 2). Their origin is determined by photoemission from the O 2*p* levels of atomic adsorbed oxygen [14, 15, 17, 33, 34]. Three characteristic lines appearing in the Auger spectra of oxygen (Fig. 3) correspond to the transitions (in decreasing order of intensity): *KVV* (~513 eV), *KLV* (~490 eV), and *KLL* (~480 eV). Note that X-ray notation is traditionally applied to Auger transitions: the terms *K*, *L*, and *V* in the case of oxygen correspond to the 1*s*, 2*s*, and 2*p* spectroscopic levels. The most intense O *KVV* lines are positioned at the values of kinetic energies of 514.5 eV for O_{nucl} and 511.9 eV for O_{elec}.

The results of measurements of the corresponding spectral characteristics of nucleophilic and electrophilic oxygen and in the structure of bulk oxide Ag_2O [46] are shown in the table. Based on the values measured, we estimated the contribution of the relaxation effect to the apparent shifts of the E_b values. These data are also presented in the table.

It was found that the difference in the apparent values of the binding energies of electrons at the O 1*s* level for nucleophilic oxygen and in the composition of bulk oxide Ag_2O is largely determined by relaxation effects. The contribution of orbital energy ΔE(O 1*s*) to the overall chemical shift is 0.1 eV, which is comparable with the error in determining the position of photoelectron lines. On the contrary, the apparent chemical shift of the position of the O 1*s* level of the nucleophilic and electrophilic states, which is equal to 2.1 eV, cannot be explained only by the effects of the final state. Only 0.9 eV of the total value of a chemical shift is determined by the relaxation effect. A significant value of the "true" chemical shift (1.2 eV) is stipulated by the effect of the initial state, which points to the substantial difference in the value of the effective charge at the oxygen atoms in these forms.

Another method that enables one to estimate the charge state of an oxygen atom is based on analysis of the relative intensities and the value of the O *KVV* and O *KLV* splitting in the Auger spectra of oxygen, which, as shown above, change with a change in the extent of the ionic character in metal–oxygen bond [47, 48]. It is intuitively understandable that an increase in the effective charge at the oxygen atom or the population of the O 2*p* orbitals would differently affect the rate of relative intensities of O *KVV*, O *KLV*, and O *KLL* lines. The intensity (*I*) of the O *KVV* line is practically proportional to the population of the O 2*p* level and O *KLL*, to the population of the O 2*s* level. At the same time, a decrease in the splitting of the O *KVV* and O *KLV* bands

Experimental values of the positions of O 1*s*, O 2*p*, O *KLL*, and lines and corresponding chemical shifts for the nucleophilic and electrophilic adsorbed oxygen states

Oxygen state	O 1*s*	O 2*p*	O *KLL*	$\Delta_{O\ 1s}$	$\Delta_{O\ 2p}$	$\Delta_{O\ KLL}$	ΔR	ΔE(O 1*s*)
O_{nucl}	528.3	1.9	514.5	0	0	0	0	0
Ag_2O*	528.9	2.0	513.9	0.6	0.1	–0.6	–0.5	–0.1
O_{elec}	530.4	3.3	511.9	2.1	1.4	–2.6	–0.9	–1.2

* [46]. All values are in eV.

is observed as a result of an increase in the ionic character of the Me–O bond. For a broad range of oxygen-containing compounds with different degrees of the ionic character, the dependences of I_{KVV}/I_{KLV} on O (*KVV–KLV*) are linear [47]. Moreover, for these compounds, we observe a correlation between the values of splitting O(*KVV–KLV*) and the effective charges of atoms calculated on the basis of the Pauling electronegativity scale [47] (Fig. 4).

Analysis of experimental values of the parameters of the Auger spectra for nucleophilic and electrophilic adsorbed oxygen showed that the calculated values of I_{KVV}/I_{KLV} and O (*KVV–KLV*) fit the general dependence well (Fig. 4a). Using the correlation shown in Fig. 4b, we estimated the values of effective charges at the oxygen atoms in these sates. The effective charge with nucleophilic oxygen is ~1.65, and that with electrophilic oxygen is ~0.35 electron charge units. That is, the value of the charge transfer from metal to the adsorbate for these states differs by ~1.3 electron charge units, which correlates well with the true chemical shift of the ground level ΔE(O 1*s*) determined by us and equal to 1.2 eV (see table). Note that the values of charges for

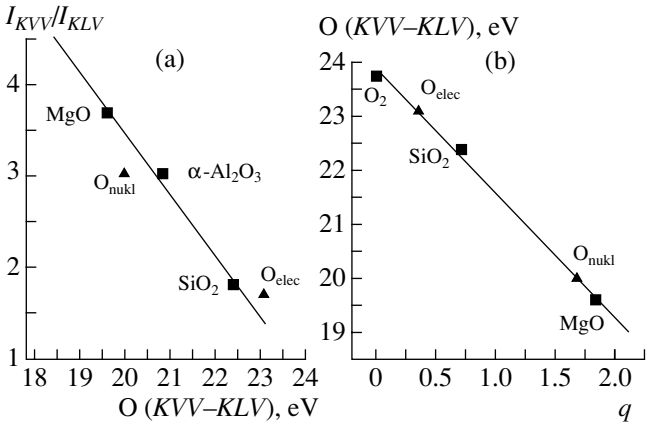

Fig. 4. (a) Correlation between the ratios of intensities of O *KVV* and O *KLV* lines (I_{KVV}/I_{KLV}) and the values of peak splitting (O (*KVV–KLV*)) for oxygen in various chemical states. (b) Dependence of the effective Pauling charge *q* [47] on the value of the oxygen Auger line splitting O (*KVV–KLV*).

both the electrophilic and the nucleophilic, oxide-like states of adsorbed oxygen differ substantially from the complete charge equal to –2, which should have been formed in the case of a purely ionic bond. The calculated value of the effective charge at the nucleophilic oxygen atom agrees well with the results of quantum chemical calculations. Thus, Martin and Hay [49], based on *ab initio* cluster calculations, predicted a high value of the charge transfer from metal to oxygen: 1.7 (Mulliken) electron charge units. It is likely that the silver–oxygen bond is covalent to a substantial degree in both cases.

This assumption is confirmed by the O *K*-edge X-ray absorption spectra (Fig. 5). The method is element-sensitive and provides direct information on vacant orbitals of atoms and molecules. In agreement with dipole selection rules ($\Delta l = \pm 1$), transitions are possible in the *K*-edge X-ray absorption spectrum, in which electron excitation from the ground O 1*s* level onto vacant O 2*p* orbitals takes place [50]. The presence of intense absorption in the spectra of nucleophilic and electrophilic oxygen shows that O 2*p* orbitals are partially vacant in both cases. This would be impossible in the case of a purely ionic bond: in the doubly charged O^{2-} ion, the electron configuration $2s^22p^6$ corresponds to the completely occupied 2*p* orbitals and the transition $1s \longrightarrow 2p$ corresponding to the O *K*-edge of X-ray absorption should formally be forbidden.

Despite the high intensity of X-ray absorption in both cases (Fig. 5), the structures of spectra of nucleophilic and electrophilic oxygen are radically different. In the XANES spectrum of the nucleophilic state, two peaks are observed: ~531 and ~539 eV (Fig. 5a). According to the literature data, the presence of a signal near the K-edge of absorption (~531 eV) points to the interaction of 4*d* electrons of silver with the 2*p* electrons of oxygen [51, 52]. A broad signal in the region of 5–10 eV behind the absorption edge assumes the hybridization of 2*p* electrons of oxygen with 5*sp* electrons of metal. An analogous XANES structure is observed for oxygen in the composition of bulk oxide Ag_2O, once again pointing to their close electron structure (Fig. 5a). The participation of 4*d* electrons of silver in the formation of the oxygen–silver bond in the case of Ag_2O is also supported by the appearance of a line

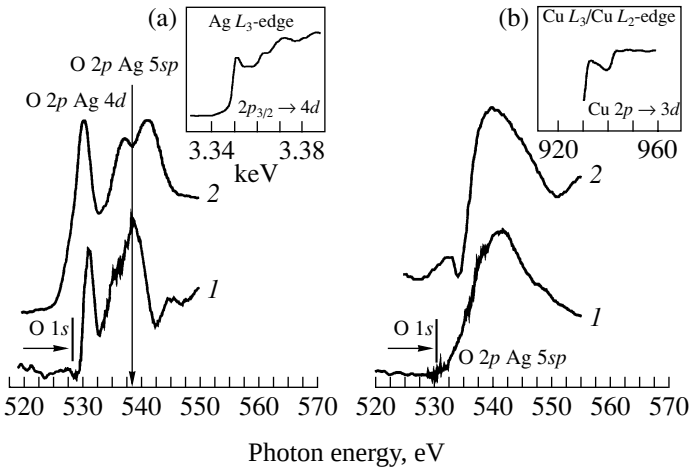

Fig. 5. The spectra of O *K*-edge absorption: (a) (*1*) nucleophilic oxygen and (*2*) Ag_2O; (b) (*1*) electrophilic oxygen and (*2*) oxygen adsorbed in the copper surface. The inserts show the spectra of (a) the *L*-edge of Ag_2O adsorption and (b) the *L*-edge of copper after oxygen adsorption.

near the Ag L_3-edge of absorption (3352 eV) corresponding to the allowed $2p_{3/2} \longrightarrow 4d$ transition, $\Delta l = 1$. An increase in its intensity correlates with an increase in the degree of the ionic character of the bond and reflects the participation of silver 4*d* electrons in the chemical interaction [53, 54]. The Ag^{1+} ion has the electron configuration $4d^{10}5s^0$. However, the formation of a chemical bond leads to the transfer of the electron density from 4*d* to 5*s* orbitals [55]. As a result, the electron configuration of silver can be described as $4d^{10-\delta}5s^{\delta}$, which determines vacant 4*d* states near the Fermi level and the appearance of the absorption band near 3352 eV.

The XANES spectrum of the electrophilic form of adsorbed oxygen contains one broad peak in the region of 541 eV (Fig. 5b). The absence of a signal near the absorption edge (~531 eV) unequivocally suggests that the 4*d* electrons of silver do not participate in the formation of the Ag–O bond of the electrophilic state. In this case the hybridization of the 2*p* electrons of oxygen with 5*sp* metal electrons only takes place.

Unfortunately we fail to find an analogy with bulk silver compounds, as was done with nucleophilic oxygen. Nevertheless, detailed analysis of published data shows that a similar XANES spectrum structure is observed in the case of the suboxide oxygen state adsorbed on the copper surface [56, 57]. In contrast to Ag_2O or CuO and Cu_2O, the XANES spectrum of copper in this case does not contain the characteristic white absorption near the *L*-edge of absorption. That is, copper atoms retain metallic properties and only 4*sp* electrons of the outer shell participate in the formation of a Cu–O bond. We may assume that, in our case, electrophilic oxygen is an adsorbed oxygen atom on the surface of metallic silver. It is known that the electron configuration of a silver atom is $4d^{10}5s^1$. In the metallic state the 5*s* electrons are delocalized in the conduction zone and, it is likely that they participate in the formation of a chemical Ag–O bond with electrophilic oxygen.

To address the question about the structure of adsorption complexes considered, we analyzed published data on the nucleophilic and electrophilic oxygen adsorbed on silver studied by structural methods on various single crystalline surfaces. Most researchers agree that the formation of nucleophilic oxygen is associated with silver surface reconstruction. Thus, oxygen adsorption on the Ag(110) plane at 300–500 K leads to the appearance of superstructures $(n \times 1)$, where *n* decreases from 7 to 2 with an increase in the O_2 exposure. This is accompanied by the appearance of the O 1*s* signal with a binding energy of 528.4 ± 0.1 eV (calibration using the Ag $3d_{5/2}$ line with E_b = 368.2 eV) [18–20, 28]. The use of STM and XRD methods were used to determine the overlayer Ag(110)-(2×1)-O structure in detail: the oxygen atoms are practically in the plane of an added row, and the length of the Ag–O bond is 2.044 Å, which practically coincides with bond length in the bulk oxide Ag_2O (2.05 Å) [23, 24]. A considerable increase in the work function, which is 0.8 eV at saturation coverage (θ = 0.5 ML), compared to the clean surface points to a significant transfer of electron density from the metal to oxygen atoms [28]. The linear dependence of the change in the work function on silver coverage by atomic adsorbed oxygen points to the independence of the dipole momentum (per one adsorbed oxygen species) of the coverage [29]. That is, the electron structure of the nucleophilic oxygen adsorbed on the Ag(110) surface is oxide-like and does not depend on the coverage.

The formation of an overlayer structure analogous to that on the reconstructed surface Ag(110)-(2×1)-O due to surface faceting occurs on the stepped Ag(331) surface [30]. Nucleophilic oxygen adsorption on the

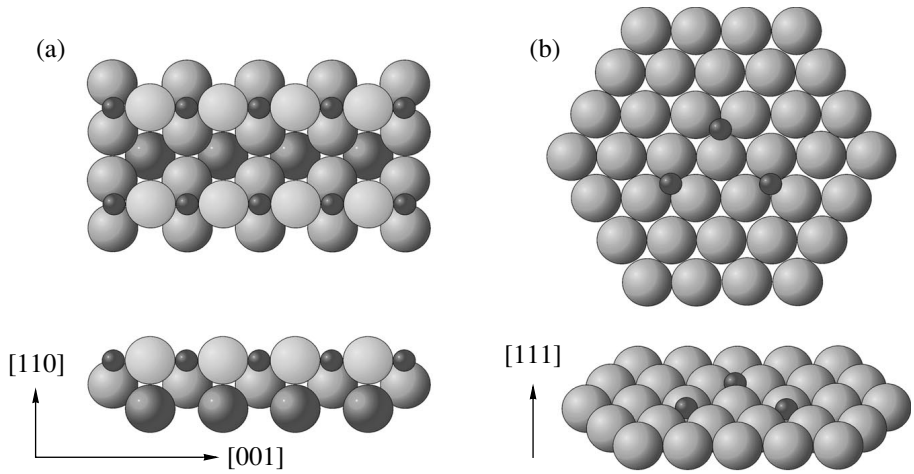

Fig. 6. The structural model of oxygen adsorption states: (a) nucleophilic oxygen on the reconstructed Ag(110) surface and (b) electrophilic oxygen on the unreconstructed Ag(111) surface.

close-packed Ag(111) surface leads to the $p(4 \times 4)$ surface reconstruction. Most researchers [19–22] believe that the Ag–O bond in this case is also close to the bond in bulk oxide Ag_2O.

Thus, nucleophilic oxygen is formed on the silver surface as a result of adsorption-assisted surface reconstruction with the formation of linear Ag–O–Ag fragments (Fig. 6a). Indeed, the Ag–O–Ag angle in structures similar to bulk Ag_2O and in the surface oxide (nucleophilic oxygen state on the silver surface) is close to 180°. Therefore, there is the possibility of a rather strong overlap of silver 4*d* orbitals with the oxygen 2*p* orbitals and substantial charge transfer. On the one hand, the pronounced ionic character of the Ag–O bond provides the transformation of silver atoms into the ionic form Ag^+, which is necessary for ethylene adsorption. On the other hand, it determines the nucleophilic properties of this state in ethylene epoxidation.

The structure of the electrophilic state has been less studied. Experimentally, it has only been confirmed that electrophilic oxygen adsorbs right on the silver surface [10, 17]. It is most likely that the formation of electrophilic oxygen occurs without surface reconstruction: an oxygen atom is localized in a hollow site (Fig. 6b). Thus, on the Ag(111) surface the state of adsorbed oxygen with a binding energy of O 1*s* of 530.1 eV was found earlier [21]. The angle-resolved XPS method confirmed the position of this oxygen on the surface, and the absence of surface reconstruction was confirmed by LEED. The absence of additional components in the Ag 3*d* spectrum points to the covalent character of the Ag–O bond for this state.

The model proposed agrees well with the results of quantum chemical calculations. The existence of a stable adsorbed atomic oxygen state was reported in [58–60] for the unreconstructed Ag(111) surface. In that case, oxygen is at the hollow site and binds to three silver atoms (the third-order axis is set by the surface symmetry). The length of the Ag–O bond is 2.109 Å (to compare, for nucleophilic oxygen it is 2.044 Å). In this case we expect a much less pronounced (compared to nucleophilic oxygen) charge transfer from the metal to adsorbate. The structure of the "oxy radical state" of adsorbed oxygen on the Ag(110) surface is similar [31, 32]. Oxygen is also localized in a threefold site of the unreconstructed surface. Thus, electrophilic oxygen is formed on the surface via dissociative adsorption without surface reconstruction. This determines the high degree of covalent character of the Ag–O bond and, accordingly, the electrophilic properties of this state in ethylene epoxidation.

CONCLUSIONS

Thus, the results of the spectroscopic study confirmed the existence of two forms of silver on the surface with different electron structures. It was found that a substantial difference in the positions of the O 1*s* lines for the nucleophilic (528.3 eV) and electrophilic (530.4 eV) states is determined by the effects of the initial state, that is, by different charge states of anions. The use of the known correlation of the Auger oxygen line splitting with the Pauling charge at the oxygen atom showed that there is a substantial difference (~1 electron charge unit) in the charge transfer from the metal to the oxygen atom in the course of adsorption with the formation of the nucleophilic and electrophilic oxygen states. Data of X-ray absorption of the oxygen *K*-edge suggest that in the nucleophilic state the Ag–O bond is formed with a substantial overlap of 4*d* and 5*sp* orbitals of silver with the 2*p* orbitals of oxygen. In the case of electrophilic oxygen, there is an overlap of silver 5*sp* orbitals and oxygen 2*p* orbitals. Comparison of experimental data with the results of theoretical calculations suggests that the charge state of oxygen in oxide

systems may substantially depend on its binding to metal atoms.

ACKNOWLEDGMENTS

This work was supported by the Russian Foundation for Basic Research (grant no. 00-15-99335).

REFERENCES

1. Kilty, P.A. and Sachtler, W.M.H., *Catal. Rev.–Sci. Eng.*, 1974, vol. 10, p. 1.
2. Sachtler, W.M.H., Backx, C., and van Santen, R.A., *Catal. Rev.–Sci. Eng.*, 1981, vol. 23, p. 127.
3. Backx, C., Moolhuysen, J., Geenen, P., and van Santen, R.A., *J. Catal.*, 1981, vol. 72, p. 364.
4. Campbell, C.T., *J. Catal.*, 1985, vol. 94, p. 436.
5. Van Santen, R.A. and de Groot, C.P.M., *J. Catal.*, 1986, vol. 98, p. 530.
6. Van Santen, R.A. and Kuipers, H.P.C.E., *Adv. Catal.*, 1987, vol. 35, p. 265.
7. Grant, R.B. and Lambert, R.M., *J. Catal.*, 1985, vol. 92, p. 364.
8. Khasin, A.V., *Kinet. Katal.*, 1993, vol. 34, no. 1, p. 42.
9. Bal'zhinimaev, B.S., *Kinet. Katal.*, 1999, vol. 40, no. 6, p. 879.
10. Bukhtiyarov, V.I., Boronin, A.I., Prosvirin, I.P., and Savchenko, V.I., *J. Catal.*, 1994, vol. 150, p. 268.
11. Bukhtiyarov, V.I., Prosvirin, I.P., and Kvon, R.I., *Surf. Sci.*, 1994, vol. 320, p. 47.
12. Boronin, A.I., Avdeev, V.I., Koshcheev, S.V., Murzakhmetov, K.T., Ruzankin, S.F., and Zhidomirov, G.M., *Kinet. Katal.*, 1999, vol. 40, no. 5, p. 721.
13. Bukhtiyarov, V.I., Kaichev, V.V., Podgornov, E.A., and Prosvirin, I.P., *Catal. Lett.*, 1999, vol. 57, p. 233.
14. Bukhtiyarov, V.I., Hävecker, M., Kaichev, V.V., Knop-Gericke, A., Mayer, R.W., and Schlögl, R., *Catal. Lett.*, 2001, vol. 74, p. 121.
15. Bukhtiyarov, V.I., Hävecker, M., Kaichev, V.V., Knop-Gericke, A., Mayer, R.W., and Schlögl, R., *Nucl. Instrum. Methods Phys. Res. A.*, 2001, vol. 470, p. 302.
16. Bao, X., Muhler, M., Pettinger, B., Schlögl, R., and Ertl, G., *Catal. Lett.*, 1993, vol. 22, p. 215.
17. Bao, X., Muhler, M., Shedel-Niedrig, Th., and Schlögl, R., *Phys. Rev. B*, 1996, vol. 54, p. 2249.
18. Campbell, C.T. and Paffett, M.T., *Surf. Sci.*, 1984, vol. 143, p. 517.
19. Campbell, C.T., *Surf. Sci.*, 1985, vol. 157, p. 43.
20. Bare, S.R., Griffiths, K., Lennard, W.N., and Tang, H.T., *Surf. Sci.*, 1995, vol. 342, p. 185.
21. Bukhtiyarov, V.I., Kaichev, V.V., and Prosvirin, I.P., *J. Chem. Phys.*, 1999, vol. 111, p. 2169.
22. Carlisle, C.I., Fujimoto, T., Sim, W.S., and King, D.A., *Surf. Sci.*, 2000, vol. 470, p. 15.
23. Taniguchi, M., Tanaka, K., Hashizume, T., and Sakurai, T., *Surf. Sci.*, 1992, vol. 262, p. 123.
24. Pascal, M., Lamont, C.L.A., Baumgartel, P., Terborg, R., Hoeft, J.T., Schaff, O., Polcik, M., Bradshow, A.M., Toomes, R.L., and Woodruff, D.P., *Surf. Sci.*, 2000, vol. 464, p. 83.
25. Rocca, M., Savio, L., Vattuone, L., Burghaus, U., Palomba, V., Novelli, N., Buatier de Mongeot, F., Valbusa, U., Gunnela, R., Gomelli, G., Baraldi, A., Lizzit, S., and Paolucci, G., *Phys. Rev. B*, 2000, vol. 61, p. 213.
26. Bukhtiyarov, V.I., Carley, A.F., Dollard, L.A., and Roberts, M.W., *Surf. Sci.*, 1997, vol. 381, p. L605.
27. Bukhtiyarov, V.I. and Kaichev, V.V., *J. Mol. Catal. A: Chem.*, 2000, vol. 158, p. 167.
28. Rovida, G. and Pratesi, F., *Surf. Sci.*, 1975, vol. 52, p. 542.
29. Engelhadt, H.A. and Menzel, D., *Surf. Sci.*, 1976, vol. 57, p. 591.
30. Marbrow, R.A. and Lambert, R.M., *Surf. Sci.*, 1978, vol. 71, p. 107.
31. Carter, E.A., and Goddard, W.A., III, *J. Catal.*, 1988, vol. 112, p. 80.
32. Carter, E.A. and Goddard, W.A., III, *Surf. Sci.*, 1989, vol. 209, p. 243.
33. Sekiba, D., Nakamizo, H., Ozawa, R., Gunji, Y., and Fukutani, H., *Surf. Sci.*, 2000, vol. 449, p. 111.
34. Savio, L., Vattuone, L., Rocca, M., De Renzi, V., Gardonio, S., Mariani, C., Del Pennino, U., Cipriani, G., Dal Corso, A., and Baroni, S., *Surf. Sci.*, 2001, vol. 486, p. 65.
35. Joyner, R.W., Roberts, M.W., and Yates, K., *Surf. Sci.*, 1979, vol. 87, p. 501.
36. Prosvirin, I.P., Tikhomirov, E.P., Sorokin, A.M., Kaichev, V.V., and Bukhtiyarov, V.I., *Kinet. Katal.*, 2003, vol. 44 (in press).
37. Kaichev, V.V., Sorokin, A.M., Timoshin, A.I., and Vovk, E.I., *Prib. Tekh. Eksp.*, 2002, no. 1, p. 58.
38. Knop-Gericke, A., Hävecker, M., Neisius, Th., and Shedel-Niedrig, Th., *Nucl. Instrum. Methods Phys. Res. A*, 1998, vol. 406, p. 311.
39. Minachev, Kh.M. and Khodakov, Yu.S., Abstracts of Papers, *XII Mendeleevskii s"ezd po obshchei i prikladnoi khimii* (XII Mendeleev Congr. on General and Applied Chemistry), Moscow: Nauka, 1981.
40. Nefedov, V.I., *Rentgenoelektronnaya spektroskopiya khimicheskikh soedinenii* (X-ray Electron Spectroscopy of Chemical Compounds), Moscow: Khimiya, 1984.
41. Wagner, C.D., *Faraday Discuss.*, 1975, no. 60, p. 291.
42. Wagner, C.D., *J. Electron Spectrosc. Relat. Phenom.*, 1977, vol. 10, p. 305.
43. Wagner, C.D., Gale, L.H., and Raymond, R.H., *Anal. Chem.*, 1979, vol. 51, p. 466.
44. Wagner, C.D., Zatko, D.A., and Raymond, R.H., *Anal. Chem.*, 1980, vol. 52, p. 1445.
45. Hohlneicher, G., Pulm, H., and Freund, H.-J., *J. Electron Spectrosc. Relat. Phenom.*, 1985, vol. 37, p. 209.
46. Tjeng, L.H., Meinders, M.B.J., van Elp, J., Ghijsen, J., Sawatzky, G.A., and Johnson, R.L., *Phys. Rev. B: Condens. Matter*, 1990, vol. 41, p. 3190.
47. Ascarelli, P. and Moretti, G., *Surf. Interface Anal.*, 1985, vol. 7, p. 8.
48. Weißmann, R., *Solid State Commun.*, 1979, vol. 31, p. 347.

49. Martin, R.L. and Hay, P.J., *Surf. Sci.*, 1983, vol. 130, p. L283.
50. Stöhr, J., *NEXAFS Spectroscopy*, Berlin: Springer, 1992, vol. 25.
51. De Groot, F.M.F., Grioni, M., Fuggle, J.C., Ghijsen, J., Sawatzky, G.A., and Petersen, H., *Phys. Rev. B* 1989, vol. 40, p. 5715.
52. Purans, J., Kuzmin, A., Parent, Ph., and Laffon, C., *Physica B*, 1999, vols. 259–261, p. 1157.
53. Behrens, P., *Solid State Commun.*, 1992, vol. 81, p. 235.
54. Behrens, P., Aßmann, S., Bilow, U., Linke, C., and Jansen, M., *Z. Anorg. Allg. Chem*, 1999, vol. 625, p. 111.
55. Deb, A. and Chatterijee, A.K., *J. Phys.: Condens. Matter*, 1998, vol. 10, p. 11719.
56. Knop-Gericke, A., Hävecker, M., Shedel-Niedrig, Th., and Schlögl, R., *Catal. Lett.*, 2000, vol. 66, p. 215.
57. Knop-Gericke, A., Hävecker, M., Shedel-Niedrig, Th., and Schlögl, R., *Top. Catal.*, 2000, vol. 10, p. 187.
58. Zil'berberg, I.L., Milov, M.A., and Zhidomirov, G.M., *Zh. Strukt. Khim.*, 1999, vol. 40, p. 422.
59. Milov, M.A., Zil'berberg, I.L., Ruzankin, S.F., and Zhidomirov, G.M., *Zh. Strukt. Khim.*, 2000, vol. 41, p. 248.
60. Milov, M.A., Zilberberg, I.L., Ruzankin, S.Ph., and Zidomirov, G.M., *J. Mol. Catal. A: Chem.*, 2000, vol. 158, p. 309.